PRL **101,** 016401 (2008) PHYSICAL REVIEW LETTERS week ending
4 JULY 2008

High-T_c Superconductivity in Superhard Diamondlike BC_5

Matteo Calandra and Francesco Mauri

CNRS and Institut de Minéralogie et de Physique des Milieux condensés, case 115, 4 place Jussieu, 75252, Paris cedex 05, France

(Received 6 March 2008; published 30 June 2008)

Using density functional theory calculations we show that the recently synthesized superhard diamond-like BC_5 is superconducting with a critical temperature of the same order as that of MgB_2. The average electron-phonon coupling is $\lambda = 0.89$, the phonon-frequency logarithmic average is $\langle\omega\rangle_{\log} = 67.4$ meV, and the isotope coefficients are $\alpha(\mathrm{C}) = 0.3$ and $\alpha(\mathrm{B}) = 0.2$. In BC_5, superconductivity is mostly sustained by concerted vibrations of the B atom and its C neighbors.

DOI: 10.1103/PhysRevLett.101.016401 PACS numbers: 71.15.Mb, 74.10.+v

Diamond is the hardest material available in nature, a very good thermal conductor and a large gap insulator. Heavily boron-doped diamond ($B_\delta C_{1-\delta}$) is superconducting at a boron content of $\delta = 0.028$ [1]. In thin films, T_c increases with δ up to 7 K [2]. These critical temperatures are lower than those of other superconducting carbon materials such as nanotubes [3] ($T_c = 15$ K), intercalated graphite compounds [4,5] ($T_c = 11.4$ K in CaC_6) and alkali-doped fullerides [6,7] ($T_c = 33$ K in $RbCs_2C_{60}$). Thus, hole doping of diamond does not look very promising for high T_c superconductivity. However, very recently, superhard nanocrystalline aggregates of BC_5, corresponding to *B*-content of $\delta = 0.166$ were synthesized [8]. In addition to being a superhard material, harder than *c*-BN, BC_5 is interesting since the introduction of such a massive number of carriers in diamond can induce strong scattering between holes and hard phonon modes.

At low B content ($\delta \approx 0.02$–0.06), density functional theory (DFT) calculations based on a supercell approach [9–11] have shown that superconductivity is phonon mediated with holes scattering to high energy optical phonon modes. The contributions of the acoustic modes is negligible. Most surprisingly, B-phonon states play a major role in the coupling to optical modes, despite the low B concentration. Moreover a Löwdin population analysis shows that the electronic states at ϵ_f are mainly of B character [9]. This is contrary to what happens in rigid band doping [12] or in a virtual crystal approach [11,13,14].

The coupling to hard optical phonons generates a large electron-phonon matrix element. However, at low doping, the average electron-phonon coupling λ and T_c are small because of the low number of carriers. Indeed the increase of T_c with doping observed in thin films [2] is mainly to due the increase in the density of states (DOS) [10] at the Fermi level.

These findings are valid at dopings of the order of some percents, but are questionable at dopings as large as those of BC_5. First of all, it is not clear at large doping how much the number of carriers can increase, since a rigid band picture fails and the results depend on the fine details of the DOS. Furthermore, if many electronic states are allowed to couple to phonons generating a considerable electron-phonon coupling, the system can be driven to a charge density wave insulator. Thus the occurrence of superconductivity in BC_5 cannot be inferred from low doping results.

In this Letter, using density functional theory calculations, we demonstrate that BC_5 has a critical temperature of the same order of that of MgB_2 [15].

Cubic BC_5 occurs as nanocrystalline aggregates [8]. The crystal structure has, on average, cubic symmetry with volume per atom of 6.00 Å^3. This value is 6% larger than the diamond volume per atom, 5.67 Å^3. Because of their similar atomic numbers, diffraction cannot distinguish between B and C atoms and consequently the position of B in the cell is not determined. In order to resolve the BC_5 crystal structure we start with the 6 atoms hexagonal supercell of the 2 atoms diamond cell. The hexagonal supercell is compatible with a cubic symmetry for $c/a = \sqrt{6} \approx 2.45$. The diamond theoretical equilibrium structure has $a = 2.529$ Å. Then we replace a C atom with a B atom and we perform volume and force optimization [16]. The results are reported in Table I. We find $a = 2.55$ Å and $c/a = 2.50$. The theoretical volume per atom in BC_5 is 5.2% larger than in diamond, in very good agreement with experiments. The c/a found is only slightly larger than the ideal one for cubic symmetry so that the BC_5 cell can be seen as a small elongation of the cubic cell along the cubic (111) axis. The most stable

TABLE I. Reduced coordinates of the theoretically devised atomic structure of BC_5. The crystal symmetry is hexagonal with $a = 2.55$ Å and $c/a = 2.50$.

Atom type	*X*	*Y*	*Z*
B	0.0	0.0	0.0070
C	0.0	0.0	0.2592
C	1/3	−1/3	0.3386
C	1/3	−1/3	0.5816
C	2/3	−2/3	0.6646
C	2/3	−2/3	0.8999

structure is nonmagnetic. Then we consider a 12 atoms cell obtained replicating the hexagonal cell along c and consider all the possible positions for two B atoms in this supercell. We found the configuration corresponding to the 6 atoms hexagonal unit cell to be the most stable by 5 mRyd/atom.

The BC_5 and diamond (C_6) electronic structures along high energy directions in the hexagonal Brillouin zone are plotted in Fig. 1. For C_6 we used the BC_5 lattice parameters and the Fermi level refers to a rigid band doping of diamond of 1 hole per C_6 unit. As it can be seen, the electronic structure of BC_5 cannot be interpreted as rigid band doping of diamond.

In BC_5, the Fermi level ϵ_f is shifted of 2.44 eV with respect to the top of the valence band, to be compared with a shift ≈ 0.8 eV at $\delta = 0.0278$ [10]. The DOS at ϵ_f is $N(0) = 0.78$ states/eV/(6 atoms cell), 2.1 times larger than its value at $\delta = 0.0278$ [10], meaning that the number of carriers induced by B doping grows continuously without saturating even for such large δ. Löwdin population analysis demonstrates that at ϵ_f the total B DOS is $N_B(0) = 0.19$, states/eV/(6 atoms cell), slightly larger that $N(0)/6$. Thus, contrary to what happens at low doping [9], the number of carriers in B electronic states is comparable to the B content.

The BC_5 phonon dispersion [16] is shown in Fig. 2. No dynamical instabilities are seen in the phonon spectrum meaning that the crystal structure obtained with geometrical optimization is dynamically stable. No charge density wave instabilities occur in the system. Decomposition of phonon vibrations (Fig. 2) into atomic components shows that, despite B being lighter than C, the harder phonon modes (120–150 meV) are due to C vibrations. At lower energies (<100 meV) the B component in the phonon density of states (PHDOS) is from 1/3 to 1/2 of the C component.

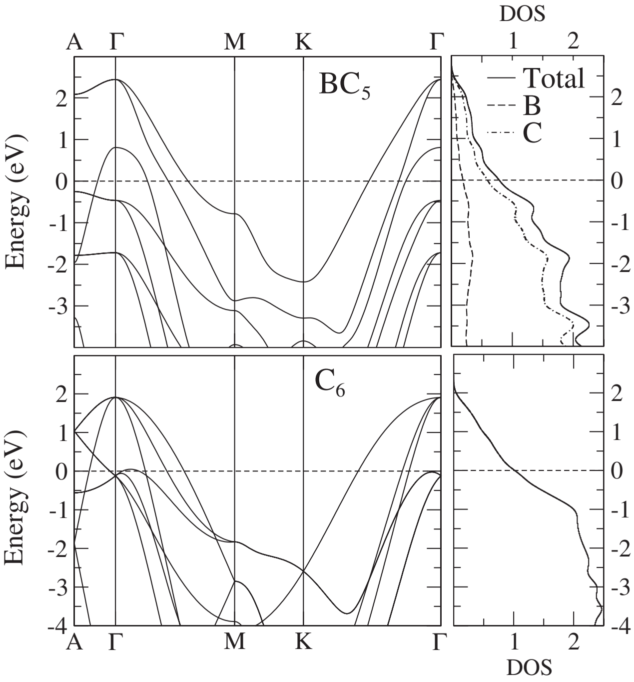

FIG. 1. BC_5 and diamond (C_6) band structure and DOS in the hexagonal Brillouin zone using the BC_5 lattice parameters. The DOS is in units of states/eV/(6 atoms cell). In C_6 the Fermi level corresponds to rigid band doping of diamond.

The superconducting properties can be understood calculating the electron-phonon coupling $\lambda_{\mathbf{q}\nu}$ for a phonon mode ν with momentum $\mathbf{q}$ and phonon frequency $\omega_{\mathbf{q}\nu}$, namely:

$$\lambda_{\mathbf{q}\nu} = \frac{4}{\omega_{\mathbf{q}\nu} N(0) N_k} \sum_{\mathbf{k},n,m} |g^{\nu}_{\mathbf{k}n,\mathbf{k}+\mathbf{q}m}|^2 \delta(\epsilon_{\mathbf{k}n}) \delta(\epsilon_{\mathbf{k}+\mathbf{q}m}), \quad (1)$$

where the summation is performed over a $N_k = 40^3$ k-point mesh in the Brillouin zone. The matrix element is $g^{\nu}_{\mathbf{k}n,\mathbf{k}+\mathbf{q}m} = \langle \mathbf{k}n | \delta V / \delta e_{\mathbf{q}\nu} | \mathbf{k} + \mathbf{q}m \rangle / \sqrt{2\omega_{\mathbf{q}\nu}}$, where V is the Kohn-Sham potential and $e_{\mathbf{q}\nu} = \sum_{A\alpha} M_A \sqrt{2\omega_{\mathbf{q}\nu}} \epsilon^{\mathbf{q}\nu}_{A\alpha} u_{\mathbf{q}A\alpha}$. $u_{\mathbf{q}A\alpha}$ is the Fourier transform of the α component of the phonon displacement of the atom A in the unit cell, M_A is the mass of atom A and $\epsilon^{\mathbf{q}\nu}_{A\alpha}$ are $A\alpha$ components of $\mathbf{q}\nu$ phonon eigenvector normalized on the unit cell.

The average electron-phonon coupling is $\lambda = \sum_{\mathbf{q}\nu} \lambda_{\mathbf{q}\nu} / N_q \approx 0.89$. Thus BC_5 is a moderate coupling superconductor with λ comparable to MgB_2. To address the role of the different vibrations in determining the electron-phonon coupling we decompose the electron-phonon coupling [19] into selected atomic vibrations, using the relation

$$\lambda = \sum_{i,j} \Lambda_{i,j} = \sum_{A,B} \left[\sum_{\alpha,\beta} \frac{1}{N_q} \sum_{\mathbf{q}} [\mathbf{G}_{\mathbf{q}}]_{A\alpha,B\beta} [\mathbf{C}_{\mathbf{q}}{}^{-1}]_{B\beta,A\alpha} \right], \quad (2)$$

where A, α ($B\beta$) indicates the displacement of the Ath (Bth) atom in $\alpha(\beta)$ Cartesian direction, $[\mathbf{G}_{\mathbf{q}}]_{A\alpha,B\beta} = \sum_{\mathbf{k},n,m} 4 \tilde{g}^*_{A\alpha} \tilde{g}_{B\beta} \delta(\epsilon_{\mathbf{k}n}) \delta(\epsilon_{\mathbf{k}+\mathbf{q}m}) / [N(0) N_k]$, and $\tilde{g}_{A\alpha} = \langle \mathbf{k}n | \delta V / \delta u_{\mathbf{q}A\alpha} | \mathbf{k} + \mathbf{q}m \rangle / \sqrt{2}$. The $\mathbf{C}_{\mathbf{q}}$ matrix is the Fourier transform of the force constant matrix (the derivative of the forces with respect to the atomic displacements). The decomposition [20] leads to the following matrix ($\lambda = \sum_{i,j} \Lambda_{i,j}$):

$$\mathbf{\Lambda} = \begin{array}{c} \\ \mathrm{B} \\ \mathrm{C}' \\ \mathrm{C}'' \end{array} \begin{array}{c} \begin{array}{ccc} \mathrm{B} & \mathrm{C}' & \mathrm{C}'' \end{array} \\ \begin{pmatrix} 0.50 & -0.18 & 0.04 \\ -0.18 & 0.69 & -0.07 \\ 0.04 & -0.07 & 0.12 \end{pmatrix} \end{array} \quad (3)$$

where C′ stands for the first two C nearest neighbors of the B atom, and C″ stands for the other three C atoms in the cell. The dominant contribution to the electron-phonon coupling comes from the vibrations of the B atom and its C neighbors.

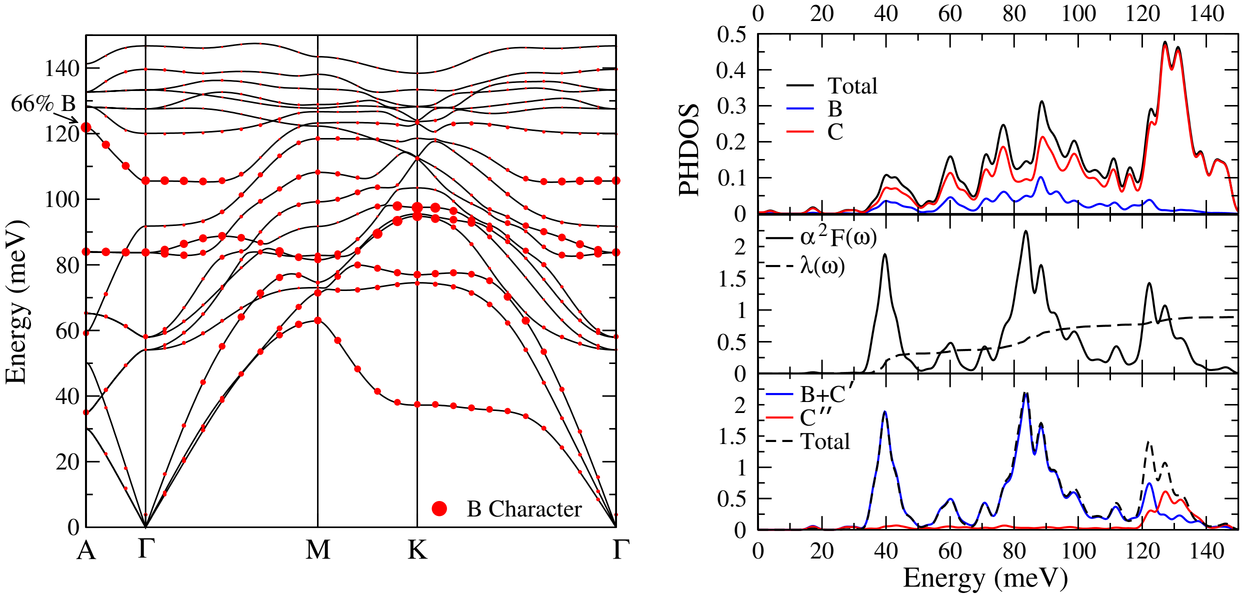

FIG. 2 (color online). (Left) BC_5 phonon dispersion in the hexagonal Brillouin zone. The radius of the red (or gray) dots is proportional to the B content of the branch. (Right) BC_5 Phonon density of states projected over B and C states, Eliashberg function $\alpha^2F(\omega)$ and integrated electron-phonon coupling $\lambda(\omega)$. The Eliashberg function has been decomposed in contributions due to vibrations of B and its C neighbors (BC′) and to vibrations of the remaining C atoms in the cell (C″).

The Eliashberg function

$$\alpha^2F(\omega) = \frac{1}{2N_q}\sum_{\mathbf{q}\nu}\lambda_{\mathbf{q}\nu}\omega_{\mathbf{q}\nu}\delta(\omega-\omega_{\mathbf{q}\nu}) \qquad (4)$$

and the integral $\lambda(\omega) = 2\int_0^\omega d\omega'\alpha^2F(\omega')/\omega'$ are shown in Fig. 2. $\alpha^2F(\omega)$ is composed of three main peaks. This is different from the low doping case [11] since in BC_5 the high energy modes (80–90 meV and 130 meV) are softer due to higher doping and the low energy modes ($\approx$40 meV) are significantly coupled (at low doping the coupling is very weak).

We also decompose α^2F as

$$\alpha^2F(\omega) = \sum_{A,B}\alpha^2_{A,B}F(\omega) = \sum_{A\alpha,B\beta}\left[\frac{1}{N_\mathbf{q}}\sum_\mathbf{q}\frac{[G_\mathbf{q}]_{A\alpha,B\beta}[L_\mathbf{q}]_{B\beta,A\alpha}}{2\sqrt{M_AM_B}}\right], \qquad (5)$$

where $[L_\mathbf{q}]_{B\beta,A\alpha} = \sum_\rho \epsilon^{A\alpha}_{\mathbf{q}\rho}\frac{\delta(\omega-\omega_{\mathbf{q}\rho})}{\omega_{\mathbf{q}\rho}}(\epsilon^{B\beta}_{\mathbf{q}\rho})^*$. Then we plot the decomposition of $\alpha^2F(\omega)$ into vibrations of B and its first two C nearest neighbors (BC') and vibrations of the other three C atoms in the cell (C″). As it can be seen in Fig. 2, the contribution of the highest energy mode (115–160 meV), essentially due to vibrations of the C-C bonds, to the electron-phonon coupling is ≈ 0.13. This is half of the contribution of the high energy structure to λ in doped diamond at $\delta = 0.018$ (from the inset of Fig. 3 in Ref. [11] one can infer that the contribution of the lower energy modes is ≈ 0.09), indicating that in BC_5 substantial weight is shifted at low energy. At lower energies, the other two main peaks in $\alpha^2F(\omega)$ are entirely due to B and its C neighbors. Further decomposition of $\alpha^2F(\omega)$ onto vibration of B and C atoms (not shown) indicates that the two low energy peaks are due to phonon modes with concerted movements of BC atoms. Thus, despite the lowest B concentration, the contribution of vibrations associated to the B atom and its neighbors are the main responsible for superconductivity.

The critical superconducting temperature is estimated using the McMillan formula [21],

$$T_c = \frac{\langle\omega\rangle_{\log}}{1.2}\exp\left[-\frac{1.04(1+\lambda)}{\lambda-\mu^*(1+0.62\lambda)}\right], \qquad (6)$$

where μ^* is the screened Coulomb pseudopotential and $\langle\omega\rangle_{\log} = \exp[\frac{2}{\lambda}\int_0^{+\infty}\alpha^2F(\omega)\log(\omega)/\omega d\omega]$ is the phonon frequencies logarithmic average. We obtain $\langle\omega\rangle_{\log} = 67.4$ meV, to be compared with 105 meV in doped diamond at $\delta = 0.0278$ [10] and 62 meV in MgB_2 [22]. The reduction in $\langle\omega\rangle_{\log}$ as compared to hole-doped diamond is due to (i) activation of coupling to low energy modes which are very weakly coupled in *B*-doped diamond and (ii) softening of the high energy modes due to the larger doping. As demonstrated, BC_5 has a 2 times larger number of carriers than doped diamond at $\delta = 0.0278$ and the phonons coupled to electrons are less energetic. Since $\lambda_{\mathbf{q}\nu}$ is proportional $N(0)/\omega^2_{\mathbf{q}\nu}$, both of these effects cooperate in increasing λ.

Using the same value of $\mu^* = 0.1$ necessary for hole-doped diamond in order to obtain $T_c = 4$ K [10] we obtain $T_c = 45$ K, which is larger than the experimentally measured 39 K in MgB_2 [15] and puts BC_5 in the class of high T_c superconductors. As in MgB_2, the T_c could be further increased by multiband effects [23].

The mutual relevance of B and C phonon modes in sustaining superconductivity in BC_5 can be addressed measuring the isotope effect coefficients for a given atomic specie $X = \mathrm{B}, \mathrm{C}$, namely $\alpha(X) = -(d \log T_c / dM_X)$. We obtain $\alpha(\mathrm{C}) = 0.3$ and $\alpha(\mathrm{B}) = 0.2$, confirming the important role of B-phonon modes.

A question arises whether the actual samples of BC_5 are able to sustain superconductivity, due to the reduced size of the grains (diameter 10–15 nm) [8]. The observation of bulk superconductivity is possible only if the coherence length $\xi_0 \sim \hbar v_F/\Delta$ is at least comparable to the size of the grains. In B-doped diamond [24], $\xi_0 = 240$ nm. Assuming parabolic bands and the same $\Delta(0)/k_b T_c = 1.78$ as in boron-doped diamond, v_f is 16 times larger and $\xi_0 \approx 400$ nm. Thus it is necessary to grow larger samples to observe bulk superconductivity in BC_5, possibly by longer synthesis or by the use of catalysts to speed up the reaction.

High energy phonon modes can lead to large T_cs even with moderate electron-phonon scattering ($\lambda \sim 0.8$–1.0), as in MgB_2. Interestingly, the quest for such a kind of high-temperature phonon-mediated superconductors coincides with that of metallic superhard materials. Superhard materials have large elastic constants, requiring short and strong chemical bonds, typically found in light-element compounds. These conditions result in energetic phonon modes. Thus high T_c superconductivity could be realized in superhard materials if doping is large enough to sustain a moderate electron-phonon coupling λ.

In this Letter we have shown that this happens in the recently synthesized [8] superhard BC_5 which is predicted to be metallic and superconducting with a $T_c = 45$ K, the largest T_c ever for a phonon-mediated superconductor.

We acknowledge discussions with Yann le Godec and M. d'Astuto and A. Gauzzi. Calculations were performed at the IDRIS supercomputing center (Project No. 081202).

[1] E. A. Ekimov *et al.*, Nature (London) **428**, 542 (2004).
[2] E. Bustarret *et al.*, Phys. Rev. Lett. **93**, 237005 (2004).
[3] Z. K. Tang *et al.*, Science **292**, 2462 (2001).
[4] T. E. Weller *et al.*, Nature Phys. **1**, 39 (2005).
[5] N. Emery *et al.*, Phys. Rev. Lett. **95**, 087003 (2005).
[6] A. F. Hebard *et al.*, Nature (London) **350**, 600 (1991).
[7] K. Tanigaki *et al.*, Nature (London) **352**, 222, (1991).
[8] V. L. Solozhenko, D. Andrault, O. O. Kurakevych, Y. Le Godec, and M. Mezouar (unpublished).
[9] X. Blase, Ch. Adessi, and D. Connétable, Phys. Rev. Lett. **93**, 237004 (2004).
[10] H. J. Xiang *et al.*, Phys. Rev. B **70**, 212504 (2004).
[11] F. Giustino *et al.*, Phys. Rev. Lett. **98**, 047005 (2007).
[12] K. W. Lee and W. E. Pickett, Phys. Rev. Lett. **93**, 237003 (2004).
[13] L. Boeri, J. Kortus, and O. K. Andersen, Phys. Rev. Lett. **93**, 237002 (2004).
[14] Y. Ma *et al.*, Phys. Rev. B **72**, 014306 (2005).
[15] J. Nagamatsu *et al.*, Nature (London) **410**, 63 (2001).
[16] Density functional theory calculations [17] were performed in the generalized gradient approximation [18] using norm-conserving pseudopotentials and a 65 Rydberg cutoff. The electronic integration is performed using a $14 \times 14 \times 14$ k-point mesh and a 60 mRyd Hermite-Gaussian smearing of order 1. The phonon dispersion is obtained by Fourier interpolation of the dynamical matrices calculated over a $4 \times 4 \times 4$ k-point mesh.
[17] http://www.pwscf.org; S. Baroni *et al.*, Rev. Mod. Phys. **73**, 515 (2001).
[18] J. P. Perdew, K. Burke, and M. Ernzerhof, Phys. Rev. Lett. **77**, 3865 (1996).
[19] M. Calandra and F. Mauri, Phys. Rev. Lett. **95**, 237002 (2005); M. Calandra and F. Mauri, Phys. Rev. B **74**, 094507 (2006).
[20] To obtain the matrix $\mathbf{\Lambda}$ in Eq. (3) we consider a 3×3 reduced matrix obtained summing over the contribution of the two C nearest neighbors of the B atom (C') and the other 3 C atoms (C'').
[21] W. L. McMillan, Phys. Rev. **167**, 331 (1968).
[22] Y. Kong *et al.*, Phys. Rev. B **64**, 020501(R) (2001).
[23] A. Liu *et al.*, Phys. Rev. Lett. **87**, 087005 (2001); H. J. Choi *et al.*, Phys. Rev. B **66**, 020513 (2002); I. I. Mazin *et al.*, Phys. Rev. B **69**, 056501 (2004); A. Floris *et al.*, Phys. Rev. Lett. **94**, 037004 (2005).
[24] B. Sacépé *et al.*, Phys. Rev. Lett. **96**, 097006 (2006).